A Photographic Method for Measuring the Angular Distribution in the Yield of Nuclear Reactions

Thesis by Sylvan Rubin

In Partial Fulfilment of the Requirements

for the Degree of Doctor of Philosophy

California Institute of Technology

Pasadena, California, 1947

Summary

A scattering camera was designed and constructed to measure the angular distribution of heavy charged particles emitted from nuclear reactions by means of the tracks which they produce in a photographic emulsion. It uses a single 2" x 4" plate to detect particles emitted in the angular range of 25° to 160° to the direction of the incident beam of bombarding particles.

The camera has been used to investigate the angular distribution of the alpha particles from the reaction $Li^7(p,\alpha)\alpha$; the long-range alpha particles from $F^{19}(p,\alpha)O^{16}$; and the resonance scattering of protons at the γ-ray levels in $Be^9(p,\gamma)B^{10}$. These reactions have been investigated over bombarding proton energies covering the range of interest in each reaction.

This apparatus has been found to be effective for detailed measurements of angular distributions, with very high resolution of energy and of angle, even for reactions with very low yield. Solid targets have been used to obtain maximum efficiency and convenience. Fogging of the plates by soft X-rays from the target has been eliminated by suitable thin target supports.

Some results and conclusions concerning the above reactions are reported.

Introduction:

The angular distribution in the yield of particles emitted in a nuclear reaction was at first measured to check the accuracy of total yield determinations. It had been assumed that the total yield could be correctly obtained from measurement of the yield within a known solid angle in any direction, and the earliest measurements of angular distribution were intended primarily to test this assumption. Kirchner [1] made the first measurement of the angular distribution of the alpha-particles from $Li^7(p,\alpha)\alpha$ in 1933, using a cloud-chamber and a transformer-rectifier set. Later, Giarratana and Brennecke [2] investigated the same reaction at 200-240 kev, using an ionization chamber detector, and also found it isotropic within their experimental error.

The first discovery of an anisotropic distribution was made by Kempton, Browne, and Maasdorp in 1936 [3], in the reaction:

$$H^2 + H^2 \longrightarrow \begin{cases} He^3 + n \\ H^3 + H^1 \end{cases}$$

They investigated both the neutrons and the protons at both 100 and 200 kev bombarding energy, finding the same angular distribution for both, with the yield forward or backward about 1.5-1.7 times as great as at 90° to the incident beam, and symmetric about 90° in center-of-mass coordinates. A high-pressure helium-filled ionization chamber was used as a detector for the neutrons, and a proportional counter for the protons. No variation with bombarding energy was observed; however, this work was done with thick targets, which minimized the variation.

In 1937, 1938, and 1939, the two reactions above, and also:

$$Li^6 + H^2 \longrightarrow 2He^4$$
$$\searrow\ Li^7 + H^1$$
$$Li^6 + H^1 \longrightarrow He^4 + He^3$$
$$B^{11} + H^1 \longrightarrow Be^8 + He^4$$
$$\searrow\ 3\ He^4$$

were investigated by a number of workers.[4, 5, 6, 7, 8, 9, 10] Neuert used a cloud chamber for his first experiments in 1937, but stated in 1938 that a cloud chamber was not suitable, and used proportional counters for all his later work. Indeed, in his work with proportional counters he used much thinner targets, and was thus able to obtain much better resolution of the variations of angular distribution with bombarding energy. All the other workers used proportional counters or ionization chambers in order to attain sufficient counting efficiency.

It was realized by this time that the determination of angular distributions provided important information on the characteristics of the quantum states involved in nuclear reactions. If the distribution is not isotropic, then both the initial and the final states must have non-zero orbital momentum, and the compound nucleus have non-zero total angular momentum. If the distribution is isotropic, then at least one of these three momenta is zero. The theory of the calculation of angular distributions of resonance reactions is treated in several papers.[11,12,13,14] The possibility of obtaining valuable clues for the assignment of quantum numbers to excited states of various light nuclei, for the development of nuclear spectroscopy, led to more careful experiments being undertaken.

Most of the previous work had been done with thick targets. The use of thin targets, which would make possible accurate measurements

of the variation of angular distribution with energy, also reduced the yield, so that it became imperative to obtain the maximum possible counting efficiency for a given angular resolution. Also, the need for energy resolution limited the possible types of particle accelerators to electrostatic generators, which deliver a very small ion current; or to transformer-rectifier sets, which give only a few hundred kilovolts, where yields are low. In order to get significant and consistent results, the statistical errors must be reduced to a few per cent, at most. This means that many counts must be obtained at each of several angles at each energy. With high resolution of angles and bombarding energy, the yield is often so low as to require a very long operating time for an experiment.

Up to now, 3 reactions have been investigated over a few hundred kev energy range with high resolution, using thin targets. $H^2(d,p)H^3$ has been done up to 400 kev, by Huntoon, Ellett, Bayley, and Van Allen in 1940 [15], and by Manning, Huntoon, Myers, and Young in 1942. [16] The distribution has been found to be fitted by the function: $(1 + A \cos^2 \theta)$ at all energies, where A increases slowly and smoothly with energy up to about 1.5 at 400 kev.

The reaction $H^2(d,n)He^3$ has been measured from 500 kev to 1.8 Mev by Bennett, Mandeville, and Richards, in 1942 [17], by using a methane-filled ionization chamber to detect the neutrons. The curve of A vs. energy was found to fit smoothly to that for the protons from $H^2(d,p)H^3$, going to about 3.3 at 1.8 Mev.

The reaction $Li^7(p,\alpha)\alpha$, once considered isotropic, has been investigated up to 1.4 Mev. It also fits the distribution function, $1 + A \cos^2 \theta$, at all energies; however, A reaches a maximum of about 2.1 at about 800 kev, and then slowly decreases. Measurements were made in 1940 up to 400 kev by Young, Ellett, and Plain [18], using multiple ionization chambers, and to 900 kev by Swartz, Rossi, Jennings, and Inglis in 1944 [19] using multiple photographic plates. This was the first use of photographic emulsion for the measurement of angular distribution. However, the plates were used in such a way as to be not more efficient than multiple ionization chambers. A plate mounted behind each of 5 foil windows detected all the particles coming through each window, but the window determined the angle and defined the solid angle of detection.

The same two pieces of apparatus used above for $Li^7(p,\alpha)\alpha$, were also used for the reaction:

$$F^{19} + H^1 \longrightarrow O^{16} + He^4$$

detecting the long-range alphas corresponding to the ground state of O^{16}. With the first (ionization chambers) apparatus, McLean, Ellett, and Jacobs in 1940[20] measured the distribution at 330-430 kev, using a thin target, and found, for the first time, an anisotropic distribution which was not symmetric about 90°, there being more yield forward than backward. Rossi and Swartz [21], using their 5 plate scattering camera in 1944, made measurements from 500-900 kev, but with thick targets, so that they were unable to obtain the angular distribution curves, but did show that there was a rapid variation of the angular distribution with energy. They could not use thin targets because of the low yield of this

reaction, such that sufficient bombardment of a thin target fogged the plates with soft radiation from the target backing.

These two reactions: $Li^7(p,\alpha)\alpha$, and $F^{19}(p,\alpha)O^{16}$ have been investigated with thin targets up to 1.4 Mev with the apparatus to be described. In addition, some work has been done on the scattering of protons from thin beryllium foils at around 1 Mev, to see whether the two $Be^9(p,\gamma)B^{10}$ resonances would influence the angular distribution of the scattering.

Apparatus:

This "scattering camera" is partly based on the design published by Chadwick, May, Pickavance, and Powell [22], which was a single plate scattering camera for use in measuring the angular distribution of scattering of high energy particles from a cyclotron on a gas target. Its chief feature was the use of a single plate, so as to take advantage of the property of an emulsion of not only integrating the yield of heavy ionizing particles, but of defining their position of impact with the emulsion, and therefore their direction of travel from a sufficiently small source. This feature greatly increases the efficiency of a photographic plate over ionization chambers for a given angular resolution. Because both the solid angle subtended by the target at the chamber aperture, and that subtended by the chamber aperture at the target must be small, the yield will be inversely proportional to the square of the

angular resolution for ionization chambers, or counters; whereas it is inversely proportional to the first power of the resolution for photographic plates used in this way, since there is no restriction on the solid angle subtended by the plate at the target.

The camera which we constructed uses a single plate in a similar manner as that of Chadwick's; however, to obtain still greater efficiency, it was decided to design it to use solid targets for either disintegration or scattering experiments, rather than the "tubular" gas target, in which energy loss in the consecutive axial elements contributing to the yield at each corresponding angle is accumulative. In a thin solid target, there is only one element, supplying particles at all angles, and thus much less energy loss for a given yield, or conversely more yield for a given energy resolution and angular resolution.

For ease of construction, the camera is a shallow cylindrical tank, about 6" in diameter, and $1\frac{1}{2}$" deep, made of 1/8" wall brass pump liner, with 3/8" thick brass covers in which rubber gaskets are recessed. Six bolts, spaced uniformly around the exterior, clamp the two covers together to make the tank vacuum tight. The axis of the target mounting assembly and collimating tube, is 1" off center, as indicated in the drawing, in order to allow sufficient space at one side for the plate-holder. Two brass blocks, after being brazed to the exterior of the cylinder, were coaxially bored on a milling machine, and close-fitting circular flanges were soldered into these blocks, so as to maintain accurate alignment. A reamed hole through each of these blocks for two of the six cover clamping bolts positively aligns the covers with respect

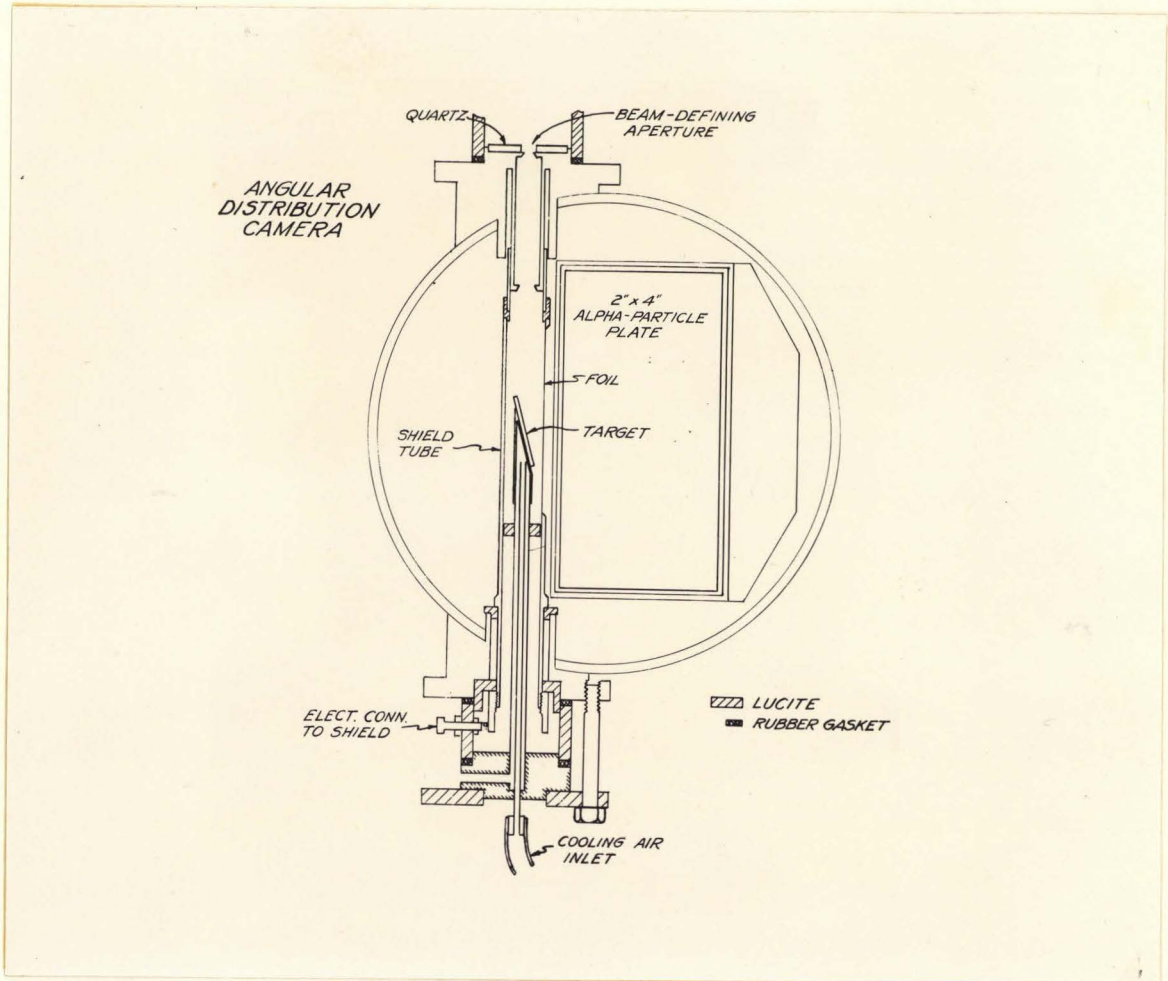

Fig. 1: Schematic drawing of scattering camera.

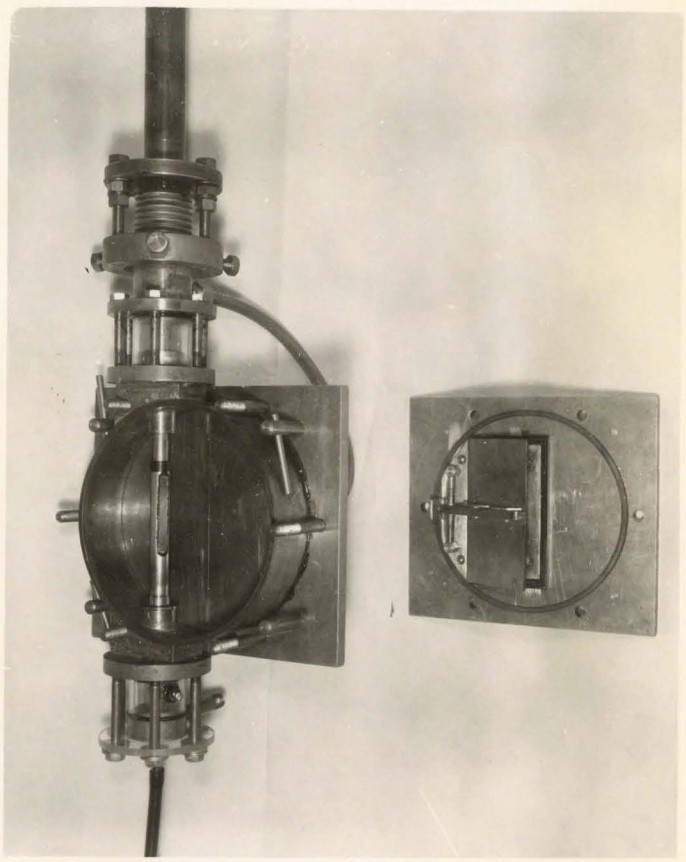

Fig. 2: Photograph of camera, showing one cover removed. Plateholder is on removed cover, with shutter in open position. Target is behind center of foil window on shield tube.

to this axis. The camera is mounted on the end of the beam analyzer of the electrostatic accelerator by means of the front flange, which also holds a tubular lucite window and the tube containing the beam defining aperture and shielding baffle aperture. On the rear flange is mounted the target assembly and shield tube.

The target is located at the central plane of the camera, on the off-center axis of the flanges. The various targets used have been mounted obliquely at 20°-25° to the incident beam, on a tubular thimble which slips on the end of a target support tube. This tube is soldered to a block which is clamped to the rear flange with lucite insulators to make possible measurements of the ion current to the target, and with rubber gaskets for vacuum seals. For the work in which thin foil targets were used, the target mounting was modified to include a quartz window cemented in the rear block, so that the ion beam, after penetrating the foil target, could be observed by the fluorescence it produced on the window. This was extremely useful in accurately aligning the beam in the camera. The target support tube is coaxial with a $\frac{1}{2}$" diameter shield tube which completely encloses it, and which is also insulated, so as to be part of a Faraday cage arrangement in which a negative potential on the shield relative to the target prevents loss of electrons from the target under ion bombardment. Into the front flange is screwed the aperture tube, with an insulated tip where it connects to the shield tube mounted on the rear flange. The aperture tube carries a quartz disc with a small hole in its center, for locating the ion beam, the beam defining aperture just below the quartz, and about $2\frac{1}{2}$" farther down, a larger aperture to prevent ions scattered by the edges of the defining aperture

from striking the electrostatic shield. The defining aperture is usually a 3/32" circular, thin-edged hole, but can be stopped down to 1/32" by an insert.

Cut in the wall of the shield tube is a rectangular slot, 1 3/4" x ¼", in which is mounted an aluminum window frame. The frame is shaped to support a curved thin aluminum foil window, 3/16" wide and 7/8" long, of 5/8" radius of curvature, in a position 5/16" from the center of the target. Various foil thicknesses are used, to stop the scattered particles of the incident beam, but allow the reaction products of longer range to penetrate to the photographic plate.

The aluminum foil window used for the earlier data on $Li^7(p,\alpha)\alpha$ was a straight, rather than curved, foil. However, the shortening of the tracks in the backward direction due to the decrease of energy in the laboratory system, combined with the increased absorption of the straight foil at large angles from the normal, gave such short tracks at large backward angles that it was difficult to measure track density in this region. Use of a curved window after the first 4 plates was a considerable improvement, although there was not sufficient space available to make its radius equal to its distance from the target. Also, by using a set of removable aluminum window frames, the window thickness could be changed more conveniently.

The photographic plates which have been used are 2" x 4" Eastman Fine-grain Alpha-particle plates, with an emulsion about 20-25 microns thick. The plates were obtained about 2 dozen at a time, and successive batches were progressively better, giving closer grain spacing

and clearer tracks. In the last emulsions used, the mean grain spacing is less than 1μ . All plates were on .043" glass, so as to be suitable for dark-field illumination with standard slide illuminating condensers. One plate is used for each run, being mounted emulsion side up in a plate holder fastened to one cover of the camera, such that the long edge of the plate is parallel to the incident beam, which was 15 mm above the plane of the emulsion. Particles from the target, after penetrating the aluminum foil window, thus strike the emulsion obliquely at about 18° along a circular arc on the emulsion at a constant distance of 50 mm from the target. From any point along this arc, between 25° and 155° to the direction of the incident beam, the entire active target is visible through the aluminum window. The plate holder is closed by a light-tight hinged shutter, which is operated from outside the camera with a lever mounted in a rubber diaphragm.

The most recent emulsions, which produce the best tracks, have such a low proportion of gelatine that there is frequent peeling of parts of the emulsion when the plate is put in a vacuum. This occurs along the edges of the plates, and sometimes quite a large piece of emulsion curls up, or breaks off. To prevent these ragged edges from projecting into the path of the particles to be detected, a clip was made of .006" shim steel, to fit snugly on the front edge of the plate. The clip extends almost to the arc along which observations are to be made, and ensures that the path to that arc from the target does not become obstructed by loose emulsion. Occasionally the peeling will cause the

loss of some data at the smallest or largest usable angles, in which cases the run is repeated if that measurement is desired.

Targets:

Considerable trouble was encountered at first with fogging of plates, even after the target had been completely enclosed to prevent escape of any scattered protons, in preliminary tests with various types of lithium and fluorine targets. It was soon found that this was due to soft X-rays from the target, as it could be eliminated by using only light elements in compounds with lithium or fluorine, and for the backing of thin targets. Thin targets of LiOH on steel or on aluminum gave excessive X-rays, but were satisfactory on a beryllium backing. A thick CaF_2 target gave considerably more fog than a thick BeF_2 target. This variation in the action of various target backing materials corresponds to the rapid increase in X-ray yield with atomic number. [23]

A run made at 700 kev, with a clean thick beryllium metal target showed no significant yield of particles through an aluminum window of 3.93 mg/cm^2 surface density, so that beryllium provides a satisfactory backing for thin targets for proton bombardment, and was used for all the work described in this paper.

All the work on $Li^7(p,\alpha)\alpha$ was done with a single target, prepared by evaporating lithium in vacuum on the surface of a small beryllium plate, and then allowing it to hydrolyze in the atmosphere to a stable LiOH film. The estimated thickness of the LiOH, determined from

the alpha-particle yield, was about 20 kev in a direction parallel to the beam, which made an angle of 22° with the target surface.

The preliminary work on $F^{19}(p,\alpha)O^{16}$ was done with a thin BeF_2 target, made by placing a drop of HF diluted with alcohol on the surface of a beryllium plate for a few seconds, then washing the excess off with alcohol. However, due to the very low cross-section for long range alphas, even this target gave excessive X-ray fogging. Although tracks were visible in it, they were difficult to count. Some targets were then made by mounting 0.5 micron thick beryllium foils on an oblique target thimble, with no backing behind the foil. The foils were coated with BeF_2 by holding a small drop of HF close to the foil for a short time. These made excellent thin targets, although fragile, requiring frequent replacement. Very satisfactory plates were obtained, with no visible fog, and easily observed tracks, in spite of the very low yield per proton.

Associated apparatus:

The camera is mounted on the end of the ion beam analyzer of the electrostatic generator, which can, under present operating conditions, go to a voltage of 1.4 Mv. For the $Li^7(p,\alpha)\alpha$ experiments, and the preliminary work on $F^{19}(p,\alpha)O^{16}$, a simple magnetic analyzer was used; for later work a combination electrostatic and magnetic analyzer was available. These analyzers, combined with an automatic electronic

voltage regulator operated by pick-up electrodes at the end of the analyzer, hold the voltage to within less than 1 kev variation, and hold the ion beam very steady in position.

The ion energy is determined by the output of a rotating sector generating voltmeter mounted in the top of the generator tank. This is calibrated with the narrow gamma-ray resonances of $F^{19}(p;\alpha,\gamma)O^{16}$ and $Be^{9}(p,\gamma)B^{10}$. In addition, since the advent of the electrostatic analyzer the analyzer deflection voltage has been found to be very convenient for ion energy determination, and is also calibrated in terms of these γ-ray resonances.

The target assembly, electrically insulated by lucite bushings, is connected to a low-leakage 1 μfd. condenser, the voltage of which is measured by a quartz fiber electrometer to give the integrated ion charge to the target. A galvanometer from the condenser to ground gives continuous readings of the instantaneous ion current.

Operation:

After the camera is mounted on the analyzer, and loaded with a plate, it is pumped out with a mechanical pump; then the gate valve in the output tube of the analyzer is opened. Usually about a half hour is required to bring the pressure down to a suitable operating vacuum for the accelerator, due to adsorbed gas and vapor in the emulsion. The shield tube is connected to -90 volts, and the voltage on the charge integrating condenser set sufficiently positive to bring the electro-

meter to the start of its scale. When the ion beam is focussed, and the accelerating voltage is steady at the desired value, the beam and camera are mutually aligned by centering the beam on the quartz disc at the entrance aperture, and adjusting the alignment for maximum target current. With the use of foil targets, this alignment is greatly simplified by centering the beam on the rear quartz window, and on the front quartz, visually. The rear quartz window also serves to provide continuous indication of the condition of the target foil during a run, since it forms a picture of any perforations in the foil.

From previous experience, and a rough estimate of target thickness, the total charge desired for some convenient track density is determined. When everything is aligned, and conditions are steady, the shutter of the plate-holder is opened; when the current integrator shows that the run is completed, it is closed.

After readmitting air to the camera, the cover on which the plate-holder is mounted is removed to a darkroom for reloading, and developing the plate. The plates are tray-developed in D-19 for 2 min. at 70° F., rinsed in stop solution, then fixed in F-5 for a little longer than required to clear. Fixing this type of emulsion takes from 15 to 30 min. to clear. They are then washed and air-dried. At the time the plates are loaded into the camera, they are numbered on the glass side with an identifying number with a china-marking pencil. This is removed after the plates are dried and numbered in one corner with ink.

Measurements:

The plates are measured on a microscope fitted with a mechanical stage, driven by a micrometer screw, and a paraboloidal dark-field illuminating condenser. Most of the observations are made with 8 power, or 40 power objectives, depending on the track density; and a 25 power hyperplane eyepiece fitted with a counting reticle, dividing the circular field of view into about 16 squares (cut off a little at the corners).

Before the plate can be measured, it is necessary to lay out a coordinate system. The plate is examined under the microscope at several positions, and adjusted each time so that the average direction of the tracks is parallel with the horizontal reticle lines, and a line is scribed on the plate through that point, also parallel with the reticle. This can be done to an accuracy of about 1°, when the tracks are of reasonable length. The plate is then clamped on a coordinate layout block, which has lines scribed at 5° intervals radiating from a punch mark. The plate is adjusted so that the convergence point (actually a small area) of the lines previously scribed on the plate, is centered on the punch mark, and the long edge is normal to the 90° line. This convergence point is about $\frac{1}{2}$" off the plate, and the adjustment is made by checking with a straightedge. Two arcs are scribed on the emulsion, at 45.7 and 49.7 mm radius about the punch mark, with a sharp pair of dividers. Since the center of the target is 15 mm above the plane of the emulsion, the center of this 4 mm wide arc is at 50 mm from the target. Radial lines are drawn on the emulsion directly above the standard lines on the layout block. The plate is then ready for counting tracks.

It is clamped on the microscope stage, and adjusted so that a radial line is parallel to the micrometer motion of the stage, and passes through the center of the field of view. Starting near one edge of the 4 mm wide arc, all tracks are counted within a rectangular swath of a little less than 4 mm in length, and some convenient width, depending on the track density. Various combinations of 8x and 40x objective, and 1, 2, or 4 squares width are used. The ratios of these widths, in actual distance, are known to about 3%, by calibration measurements on a glass reticle scale with 100 divisions, each division being 0.0916 mm. These calibration measurements were made with all available combinations of eyepieces and objectives.

From the swath dimensions, and the angle of incidence of the particles on the emulsion, the solid angle from the target is determined. For most counting, when the track density is most convenient, the 8x objective is used, and a swath 1 sq. wide (0.213 mm) and 0.140" long is counted. This, after correcting for the oblique incidence, is a solid angle from the target of 9.2×10^{-5} steradians, or 7.3×10^{-6} of a sphere. It is not difficult to count up to 1500 tracks in this area, with this magnification, or several times more, using higher magnification. However, it is most convenient to use the lower magnification, thus setting an upper limit of about 2×10^{8} emitted particles (assuming isotropic distribution) for each run. Even with thin targets, this is usually obtained with a few hundred micro-coulombs of bombarding particles.

After the counting is done at a sufficient number of different angles on the plate, depending on the detail and accuracy desired, the data is then corrected.

Corrections:

There are only three corrections required for this method of obtaining angular distributions. First, the angles measured in the plane of the plate must be converted to angles in a plane including the incident beam and the point where the tracks are observed. Since all measurements are made on an arc at 50 mm from the target, and the distance between the target and the plane of the plate is constant, this correction was computed only once and tabulated in the form of the cotangent of the corrected angle in terms of the observed angle. The formula used for this correction is:

$$\sin\theta = \frac{\sqrt{\sin^2\varphi + \left(\frac{h}{r}\right)^2}}{\sqrt{1+\left(\frac{h}{r}\right)^2}}$$

where: θ is the angle with respect to the incident beam
φ is the angle in the plane of the plate (observed)
h is the normal distance from the target to the plate
r is the radius from the target to the point of measurement.

The other two corrections are for conversion of the data in laboratory coordinates to center-of-mass coordinates, involving correcting both the angular coordinate and the yield per unit solid angle.

The correction to the angular coordinate is given by the exact expression:

$$\operatorname{ctn}\theta = \operatorname{ctn}\theta_c + \alpha \operatorname{csc}\theta_c$$

where θ is the angle in lab. coord.
θ_c is the angle in C.M. coord.

and

$$\alpha = \left[\frac{M_1 M_2 E_1}{M M_3 Q + M_0 M_3 E_1}\right]^{\frac{1}{2}}$$

where M_0 is the mass of the stationary target nucleus
M_1 is the mass of the incident nucleus
M_2 is the mass of the observed nucleus
M_3 is the mass of the residual nucleus
$M = M_0 + M_1 = M_2 + M_3$
E_1 is the energy of the incident nucleus, in lab. coord.
Q is the reaction energy

A convenient approximation, which is sufficiently accurate for this work, is:

$$ctn\,\theta_c = ctn\,\theta - \alpha\,csc\,\theta$$

Since the solid angles in which counts are made are very small in angular extent, the differential expression for the ratio of the solid angle in the C.M. system to that in the lab. system is accurate. It is:

$$\frac{d\Omega_c}{d\Omega} = \frac{\sin\theta_c}{\sin\theta}\cdot\frac{d\theta_c}{d\theta} = \frac{\left[1+2\alpha\cos\theta_c+\alpha^2\right]^{\frac{3}{2}}}{1+\alpha\cos\theta_c} \simeq 1+2\alpha\cos\theta_c$$

If N is the number of tracks in equal solid angles in the lab. system, and N_c the number in equal solid angles in the C.M. system, then

$$N_c = N + N\left(\frac{d\Omega}{d\Omega_c} - 1\right) \simeq N - N(2\alpha\cos\theta_c)$$

The use of the first approximation to the correction is sufficiently accurate, since the maximum value of in any of this work was 0.11 for proton scattering on Be^9. In this case the error in neglecting higher terms is about 2% at extreme angles. This is small compared to the statistical errors.

RESULTS

I. $Li^7(p,\alpha)\alpha$ Reaction:

The investigation of the angular distribution of the alpha particles in the reaction

$$Li^7 + H^1 \rightarrow 2He^4$$

was undertaken first, because it was desirable to use the apparatus first on a relatively simple reaction, on which previous measurements had been made. Since the products are two alpha particles, the reaction will be symmetric about 90^o in the center-of-mass system, although it is not necessarily isotropic.

Most of the plates were taken with the curved windows, using a single layer of aluminum foil of 3.93 mg/cm^2 at low bombarding energy, and two layers, or 7.86 mg/cm^2, at higher bombarding energy. These were sufficient to stop protons elastically scattered by the target and backing support.

Since the yield of this reaction is fairly high, the total proton charge to the target was of the order of 500 microcoulombs for each plate. This gave satisfactory track densities on the plates taken at medium and high energy, and about 2 - 3 times this charge at the lowest energies gave sufficient density on those plates. This bombardment was small enough so that there was no difficulty with X-ray fogging of the emulsion. The target thickness was about 20 kev, measured parallel to the proton beam. This was determined by comparing yield measurements at 545 kev with a curve based on cross-section data given by Ostrofsky, Breit, and Johnson [24], and corrected for a LiOH target, instead of Li metal.

In order to obtain good statistics, each plate was measured at many angles, counting several hundred tracks at each point, so that from 5000 to 10,000 tracks were counted on each plate (except at 1285 kev, where only 3000 tracks were counted). Thirteen plates were exposed and measured, over a range of bombarding energy from 400 to 1400 kev. The uncorrected data are given in Table 1. The original data were corrected to center-of-mass coordinates, as previously described, and the intensity was plotted as a function of $\cos^2\theta_c$. In all cases, the points could be fitted by a straight line within the experimental uncertainty, as determined by calculating the probable error of individual points on the curve, and from the mean deviation in the entire set of points for a given plate. Five of the curves are shown in Fig. 3. The resulting angular distributions are fitted satisfactorily by an expression of the form:

$$Y(\theta,E) = Y_o(E)\left[1 + A(E)\cos^2\theta_c\right]$$

where $Y(\theta,E)$ is the yield per unit solid angle, at an angle θ in the center-of-mass system with respect to the direction of the incident protons, and at a proton energy, E, measured in the laboratory system. $Y_0(E)$ is the 90^o yield function. The yield data is plotted, using 4π solid radians for unit solid angle, so that the total integrated yield in all directions is given by $Y_0(1 + A/3)$.

Fig. 4 shows the function A(E), obtained from the 13 plates tabulated. Although Swartz, et al., [19] indicated a fairly sharp maximum in A at about 700 kev, we have found only a gradual decrease above 900 kev. The value of A reaches the same maximum observed by Swartz, et al.,

Table 1

Number of tracks counted in equal areas.

φ(deg.)	E_p (kev) 360	453	545	640	730	915	920	960	1010	1155	1285	1380	1380
25	642	548	737	1084	425	695	489	742	763	539			
30	642	583	713	1023	365	660	423	728	717	524	270	1228	424
35	631				370	632				529	256		390
40	576	519	647	925	337	574	402	627	582	494	238	1118	428
45						535				457	222		348
50	570	464	548	801	299	469	314	515	532	420	212	883	347
55						432				386	185		
60	524	404	503	660	216	350	292	432	429	356	163	751	310
65						332				259			
70	474	399	461	564	183	312	227	342	319	241	121	611	217
75						282							
80	453	351	401	494	168	250	191	296	277	204	112	578	214
85						245			262				
90	455	316	369	487	169	247	177	254	329	180	112	510	205
95						237			300				
100	457	359	375	524	183	255	192	306	287	222	126	532	221
105						283							
110	482	351	416	587	185		236	337	354	279	149	632	309
115											149		
120	508	382	480	613	226	350	317	391	431	304	152	712	361
125	541		507										
130	555	436	533	691	285	417	324	449	468	335	186	795	423
135	494		516		313	444							
140	555	445		778	307	497	416	539	543		218		
145	557					515			563				
150	535	479		826		527	435	569	613		235		
155	589	501		824		545	455	568					

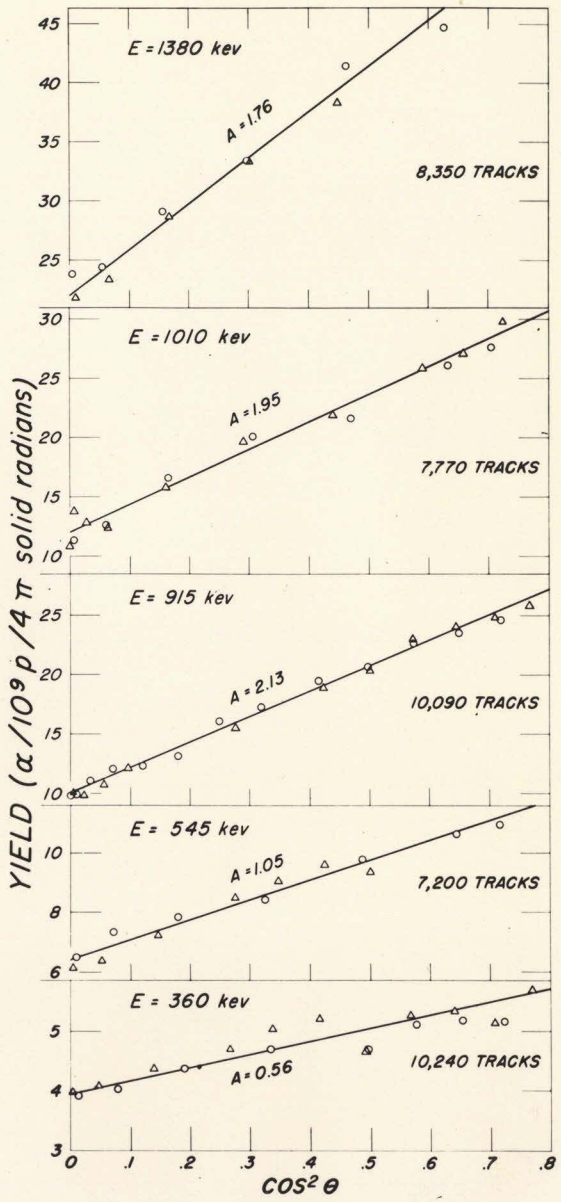

Fig. 3: Some of the angular distributions of $Li^7(p,\alpha)\alpha$, in C.M. coordinates. Circles: forward of 90°; triangles: backward of 90°.

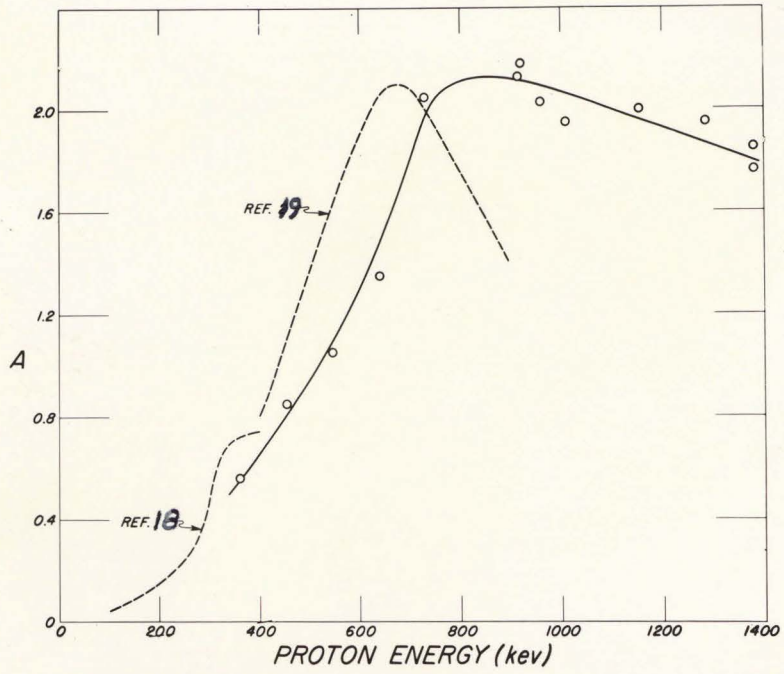

Fig. 4: Coefficient of $\cos^2\theta$ term in the angular distribution as a function of proton energy. Solid curve is fitted to our data. Dashed curves are previously published results.

but does not appear to change rapidly between 800-1400 kev.

The data which we obtained on yield per proton as a function of energy are not particularly accurate, but show no indication of any resonance, at 90°, 180°, or in total yield over the sphere, in the region up to 1400 kev. The 90° yield is a linearly increasing function up to 1400 kev in essential agreement with previous results, [24, 25] up to 1000 kev.

Dr. R. F. Christy [26] has made some calculations to relate these data on the angular distribution with the magnitude and energy dependence of the total cross section, in terms of the dispersion theory. Although the cross section is not accurately known above 0.2 Mev, it seems to show no pronounced indication of resonance from 0 to 1.4 Mev. A reasonable fit of the data is obtained with two resonances having $\Gamma = 1$ Mev at 0 and 1.8 Mev roughly. The latter is taken to have $J = 2$, but the former may be $J = 0$ or $J = 2$. If σ is normalized by the measurement of Haworth and King, [27] the proton width agrees well with that derived from the γ-ray resonance at 0.44 Mev only if the 0 energy resonance has also $J = 2$.

II. $F^{19}(p,\alpha)O^{16}$ Reaction:

Another problem investigated was the reaction $F^{19}(p,\alpha)O^{16}$, leading to the emission of 5.9 cm. alphas, and of O^{16} in its ground state. Because of the resonance character of this reaction in the energy range of 600 to 1400 kev proton energy, it was desired to investigate the angular distribution of the alphas at the various resonances, shown

in Fig. 5. [28] For this purpose it was necessary to use a sufficiently thin target to obtain adequate resolution. This reaction proved to be considerably more difficult to work with than the $Li^7(p,\alpha)\alpha$ reaction, because of the low yield. It was necessary to make considerably heavier bombardments to obtain a sufficient yield of the alpha particles, and as a result, the plates became somewhat fogged by the X-rays from the thick beryllium target backing.

However, a preliminary set of curves were obtained, although the fogging of the plates limited the extent and accuracy of the track counting. They show a considerable variation of the character of the angular distribution from one resonance to another, as is shown in Fig. 6.

Some plates were obtained later, using a different type of target. A thin foil of beryllium metal, about 0.5 μ thick, prepared by evaporation [29], was mounted on the target support, and coated with a thin film of BeF_2 by holding it in HF vapor for a short time. Much better plates were obtained with this target, which could be measured to better statistical accuracy, since they had little fogging.

Some of these were faulty, due to an obstruction in the "high energy" window, which comprised a single layer of 3.93 mg/cm^2 Al foil for the backward direction, and a double layer extending over forward angles and back to about 100° to stop the more energetic forward scattered protons. The problem of separating the alphas and the scattered protons, especially above 1 Mev, where the alphas do not have very much more range than the protons, also contributed to the difficulty of working with this reaction, since the residual range of the alphas was very short after

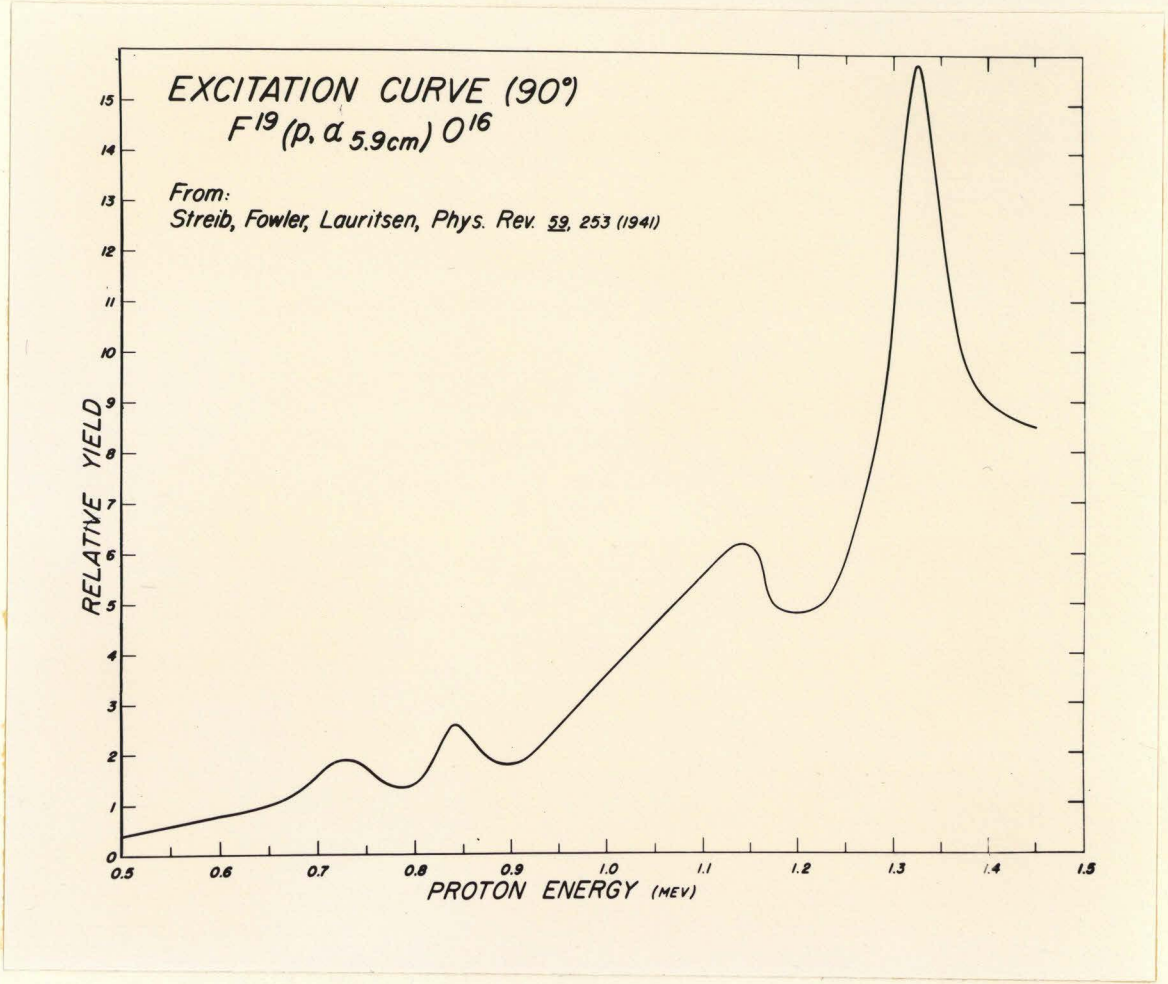

Fig. 5: Excitation curve of long range alphas from $F^{19}(p,\alpha)O^{16}$.

penetrating the foil which stopped the protons.

After a new window was prepared, two plates, at 1140 kev, and at 1330 kev were obtained. These angular distributions are shown in Figs. 7, 8. It will be noted that they essentially agree with the preliminary distributions, in indicating a very complex variation of yield with angle.

The asymmetric character of these angular distributions indicates that interference effects in the wave-function of the emitted alphas are being produced by adjacent or overlapping levels in the compound Ne^{20} nucleus, as odd powers of $\cos\theta$ in the angular distribution function can arise only from interference terms in the wave function. Also, the shapes of the distributions at small angles to the beam, where the effect of high powers of $\cos\theta$ will be significant, are such that terms of higher power than $\cos^2\theta$ appear to be needed to fit the data. If terms up to $\cos^3\theta$ or $\cos^4\theta$ are needed, this indicates an appreciable effect from d-wave incident protons.

At low energy, the shift toward higher yield in the forward direction, instead of backward, as observed at higher energies, tends to agree with McLean, Ellet, and Jacobs [20] result at 400 kev.

If we take the usually accepted spin and parity of F^{19}; that is: $\frac{1}{2}$, even, (Schiff [30] assumes $\frac{1}{2}$, odd for his recent level assignments in Ne^{20}) then we can make a tabulation of the various possibilities for the $F^{19}(p,\alpha)O^{16}$ reaction. The possible values of J (of the compound nucleus) which can lead to decay to He^4 and the ground state of O^{16} are restricted by the fact that these are both nuclei of even parity and

ANGULAR DISTRIBUTION IN $F^{19}(p,\alpha)O^{16}$

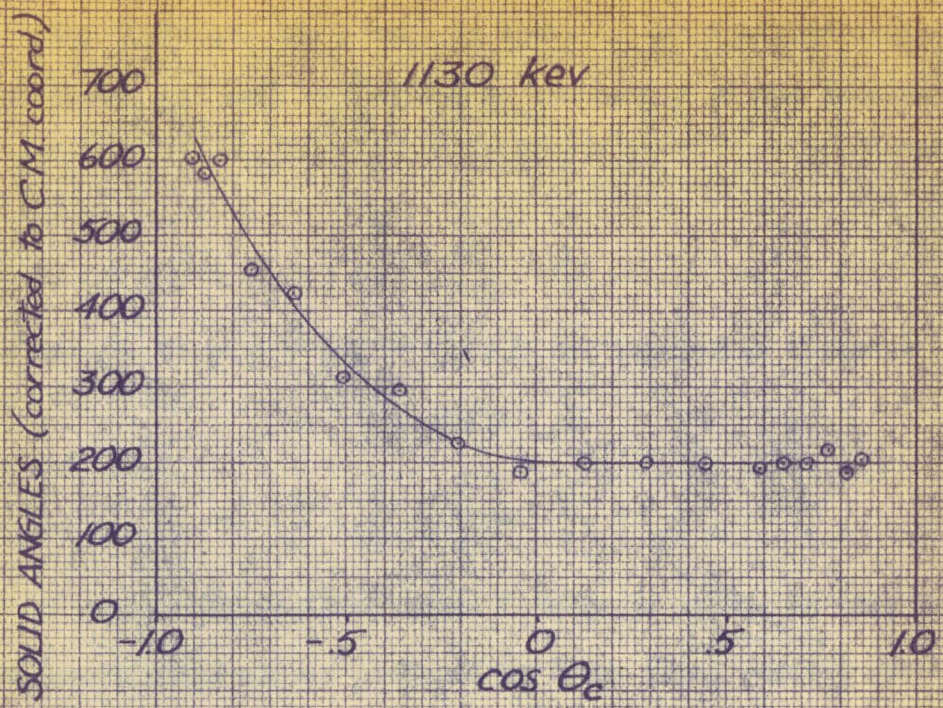

FIG. 7

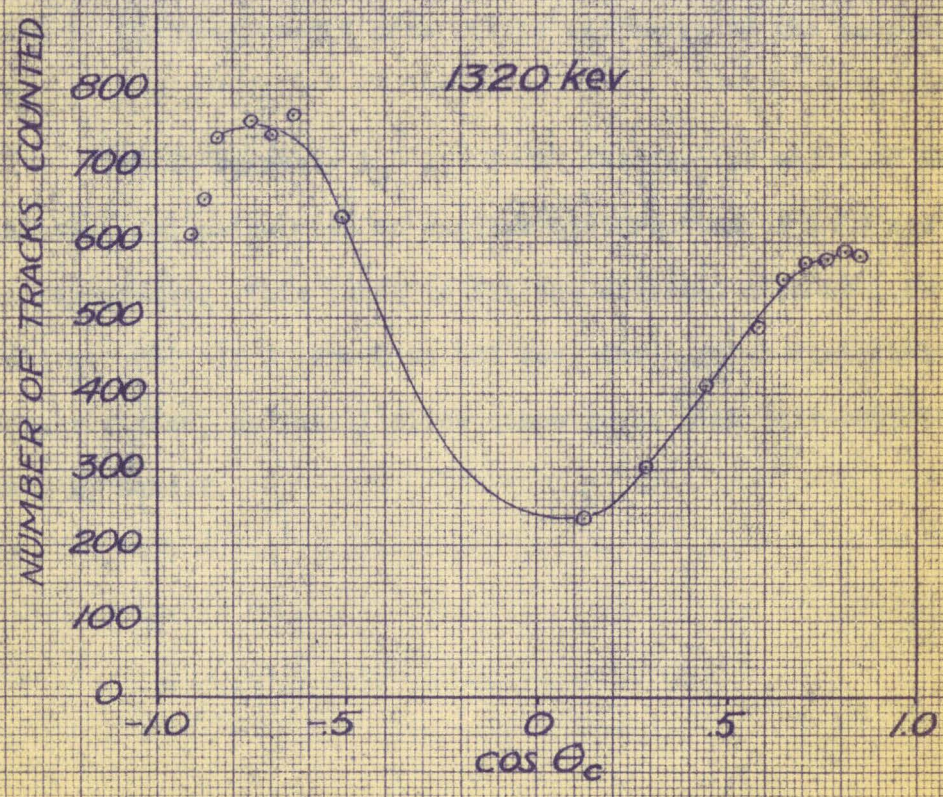

FIG. 8

zero spin; therefore the J must be equal to the relative orbital momentum in the decay, and must correspond to the parity of the compound nucleus:

L_p	Parity	J
0	even	0
1	odd	1
2	even	2

If we assume odd parity for F^{19}, then the tabulation becomes:

L_p	Parity	J
0	odd	1
1	even	0, 2
2	odd	1, 3

Since the yield of these long range alphas is very low compared to the short range alphas produced by decay to an excited state of O^{16} at about 6 Mev, it does not seem reasonable to consider the $L_p = 0$ as effective, even in the second tabulation, where L_α would be 1, since the alpha energy is well above the barrier, and the higher orbital momenta in the decay would have little influence on the long-range alpha yield.

Schiff suggests $L_p = 1$, $J = 2$ for the .83 and 1.32 Mev resonances, and calculates an angular distribution of $1 + 3\cos^2\theta$ at these resonances. This tends to fit the observed data at 1.32 Mev, but not at .83. If J were 0 at .83 Mev, the angular distribution would be better fitted, and still allow competition with pair-emission as assumed by Schiff.

III. $Be^9(p,\gamma)B^{10}$ Scattering:

It was thought that an investigation of the angular distribution of the protons scattered from Be^9 at the γ-ray resonance energies in the reaction $Be^9(p,\gamma)B^{10}$ would give some information on the reason for the difference in the character of the two prominent γ-ray resonances at 972 and 1060 kev, shown in Fig. 14. [31] The 972 kev resonance is a broad one, and the 1060 kev resonance is very narrow, suggesting that the broad one may be due to s-wave protons, and the narrow resonance to higher orbital momentum. A difference in orbital momentum might be expected to show up in the angular distribution of the resonance scattered protons at the two energies.

The chief difficulty in observing the resonance scattering is that it is combined with Coulomb scattering, and these cannot easily be considered separately, due to interference effects, especially at the angles where they are of equal magnitude. Furthermore, the reaction $Be^9(p,d)Be^8$ gives deuterons of the same range as the elastically scattered protons; and the reaction $Be^9(p,\alpha)Li^6$ yields alphas of about half their range. All the emitted particles were included in the counting, since the deuteron tracks could not, in any case, be distinguished from the proton tracks, and the alpha tracks were not easily recognizable. The very short ranges of all the particles meant that there were only about 10 grains per proton track, so that statistical fluctuations would make it difficult to distinguish them from the shorter, but more heavily ionizing, alpha tracks.

A beryllium foil, 0.23 microns thick, was used for the scattering target. It is the same thickness as the foil target used in obtaining the γ-ray excitation curve of Fig. 14. It was mounted on a .001" thick copper foil washer, with a 5/32" dia. aperture, set at 110° to the beam. The supporting thimble was cut out on one side below the target supporting washer, so that particles observed at angles smaller than 110° came from the back of the target, and those observed at larger angles, from the front. No stopping window was used, as the particle ranges were already so short that it would have been disadvantageous to try to stop the alphas, as the remaining proton range would then be so short as to make the observations difficult.

Since the cross-section for scattering is very large, an adequate yield of tracks is obtained, even from a very thin target, with a very small bombarding charge. To reduce the target current, and improve the geometry, a defining aperture of 1/32" diameter was used, with a protective baffle of 1/16" diameter, so that it was impossible for the beam to strike the copper support foil. A smaller condenser (0.1 μfd) was used in the current integrating circuit. After some preliminary runs to determine the optimum bombarding charge, it was found that 1.20 microcoulombs of protons on the 0.23 micron foil was best.

Because of the shortness of the tracks, a high magnification was more satisfactory for seeing them easily, using a 40 power objective and the 25 power eyepiece with the counting reticle. At this magnification, it was possible to count track densities as high as 20,000 tracks per sq. mm. before they became too entangled to easily distinguish

individual tracks. The exposure of the plates was adjusted to make the track density approximately 20,000 per mm^2 at around 25^o, so that the yield at large angles would be sufficient to obtain good statistics.

The results given below are based on measurements of seven plates, taken at various energies below, at, between, and above the γ-ray resonances. The first two of these were taken just after some difficulties were observed in target current measurement, which were believed to be due to residual gas pressure in the camera, as all the pumping was through the 1/32" beam defining aperture. The aperture tube was then modified to provide bypass holes for greater pumping speed before the next plates were exposed. Also the target foil was replaced with another of the same thickness after the first two plates were exposed.

Two plates at 980 kev, one made before and one after the above changes, showed no difference; however the first plate of this sequence, at 1070 kev, apparently still had something wrong with the charge measurement, as the extrapolation of the scattering yield to 0^o did not agree with any of the other plates, all of which gave an extrapolated yield of 1.0 times the calculated Rutherford scattering, while the plate at 1070 kev extrapolated to 2.0 times the Rutherford scattering. This is not surprising, since it was observed that the apparent current to the target could be changed by a large factor by varying the shield voltage at the time the 1070 kev plate was run, whereas the current was found to be independent of shield voltage on all subsequent plates.

The Rutherford scattering or protons on Be^9 was calculated from the formula:

$$n(\theta) = \frac{n_o N}{\beta}\left(\frac{10 r_o}{9E}\right)^2$$

where: n_0 is the number of incident protons
N is the number of Be atoms/cm^2
$B = (1-\cos\theta)^2 = 4\sin^4\frac{\theta}{2}$
$r_0 = 2.82 \times 10^{-13}$cm
E = proton energy in Mev.

which holds in the center-of-mass coordinate system. The tracks were counted in various areas, depending on the track density, then multiplied by an appropriate factor so that they would all correspond to an area of .140 inches length by 4 squares width (.176 mm) in the counting reticle. Calculating this solid angle, and putting it in the scattering formula, along with the beryllium foil data, the following working formula is obtained:

Rutherford scattering yield in "standard" counting area

$$= \frac{184.}{\beta E^2} \quad \text{tracks}$$

The correction of the observed angles and yield to C.M. coordinates was made on the assumption that the observed particles were elastically scattered protons, for which $\alpha = \frac{1}{9}$ (independently of E_p, since $Q = 0$). A table of correction factors for yield, and of $\cos\theta_c$, in terms of the observed angles, was prepared, and used for all the computations.

The resulting yield data was treated in several ways to see what analysis would be most suitable. The ratio of the observed yield to the calculated Rutherford scattering was plotted against $\cos\theta_c$ for

each plate. This is shown in Fig. 9. These curves show that the deviation from Rutherford scattering becomes very marked at large angles, especially at the higher energies used. Fig. 11 is a plot of the variation of this ratio with energy, taken from the smoothed curves of Fig. 9, at three angles corresponding to $\cos\theta_c = 0$, -0.5, and -0.9.

The data is also plotted as total yield minus Rutherford scattering in Fig. 10. Since the ratio to Rutherford scattering is large at large angles, the total yield at the large angles becomes more nearly equal to the additional yield, as interference effects become small, if it is assumed that the additional yield is due to resonance scattering of protons. The two wave functions will give interference terms, which will be strong where the two primary intensities are of equal magnitude, but the total yield will be not much different from the larger, when one is much stronger than the other. For this reason, the yield at large angles minus Rutherford scattering ought to be a reasonable estimate of the additional effect due either to resonance scattering, or to another reaction. The fact that these curves rise sharply at small angles indicates the probability that the increase is due to interference terms between resonance yield of protons and the Rutherford scattering, as the yield of alphas or deuterons would not show any interference effect of this sort.

Fig. 12 gives excitation curves of the resonance scattering at various angles. The points are taken from the smoothed curves of Fig. 10. They show the same sort of increase at high energy as Fig. 11, with an apparent maximum at 1000-1100 kev. This maximum may correspond to the broad γ-ray resonance at 972 kev. shown in Fig. 14. No effect of

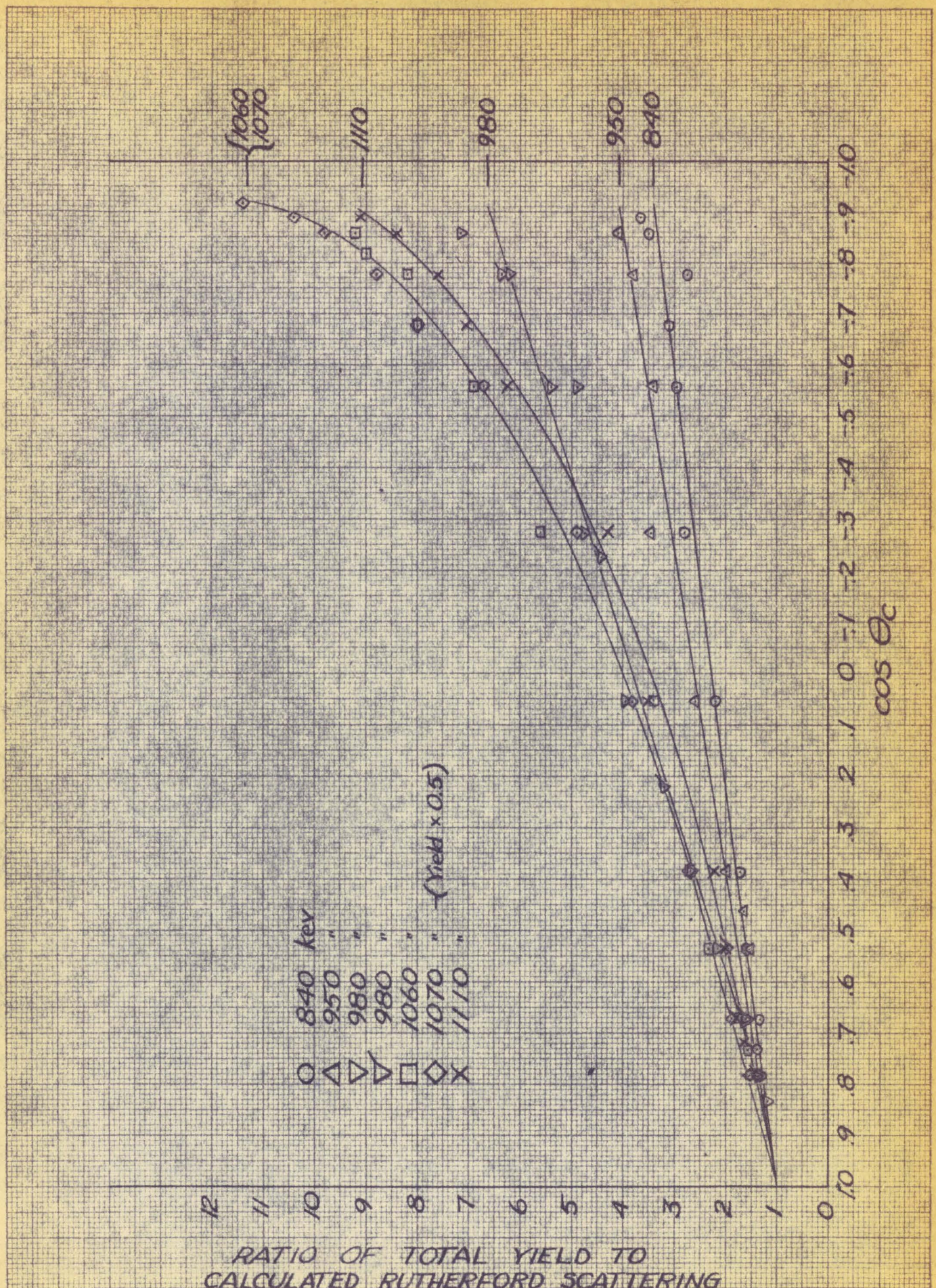
Be(p,γ)B
1060
1070
1110
980
950
840
cos θc
-1.0
-0.9
-0.8
-0.7
-0.6
-0.5
-0.4
-0.3
-0.2
-0.1
0
0.1
0.2
0.3
0.4
0.5
0.6
0.7
0.8
0.9
1.0
840 kev
950 " "
980 " "
980 " "
1060 " "
1070 " "
1110 " "
(Yield x 0.5)
12
11
10
9
8
7
6
5
4
3
2
1
0
RATIO OF TOTAL YIELD TO
CALCULATED RUTHERFORD SCATTERING

FIG. 9

$Be^9(p,\gamma)B^{10}$

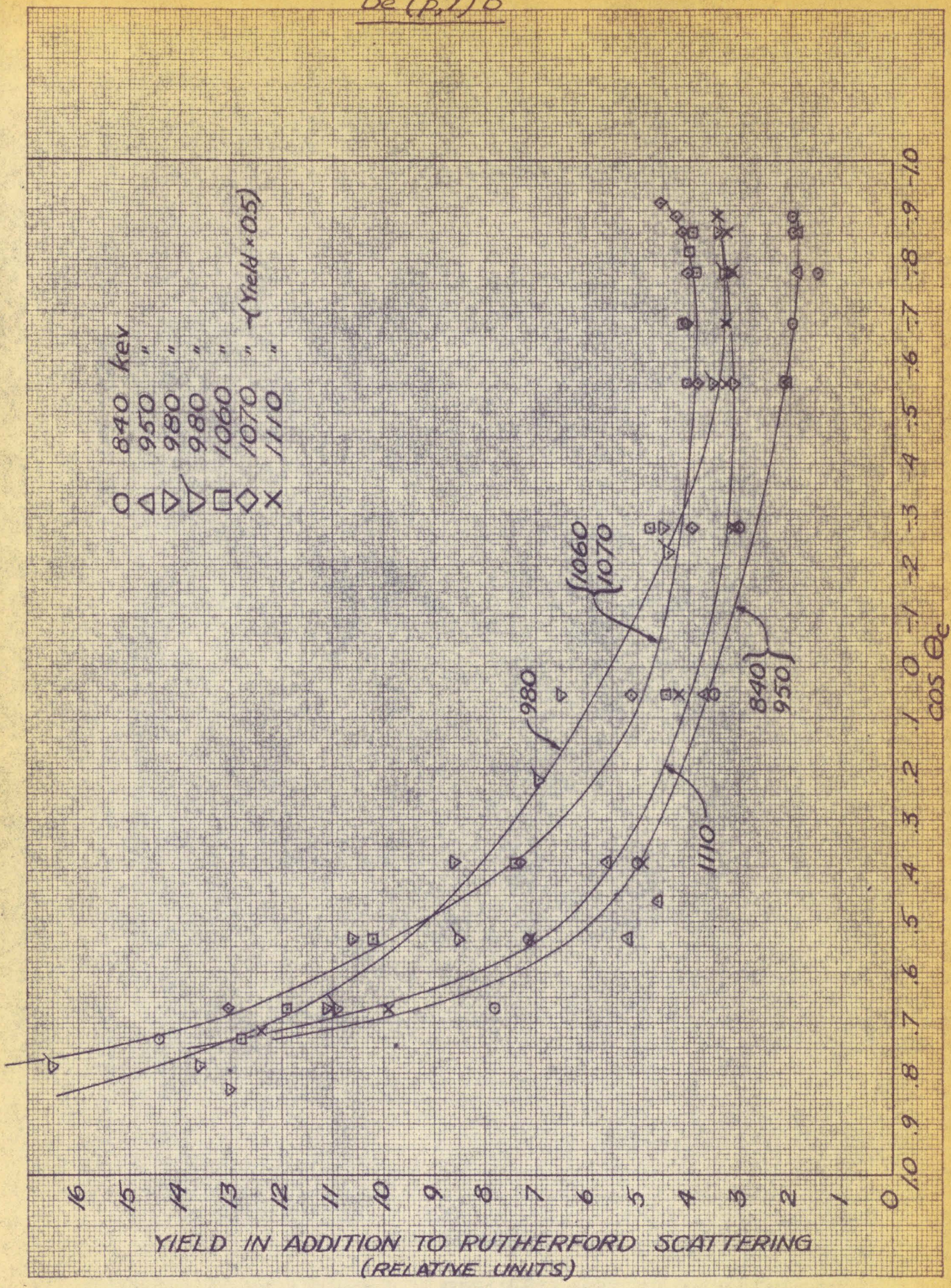

FIG. 10

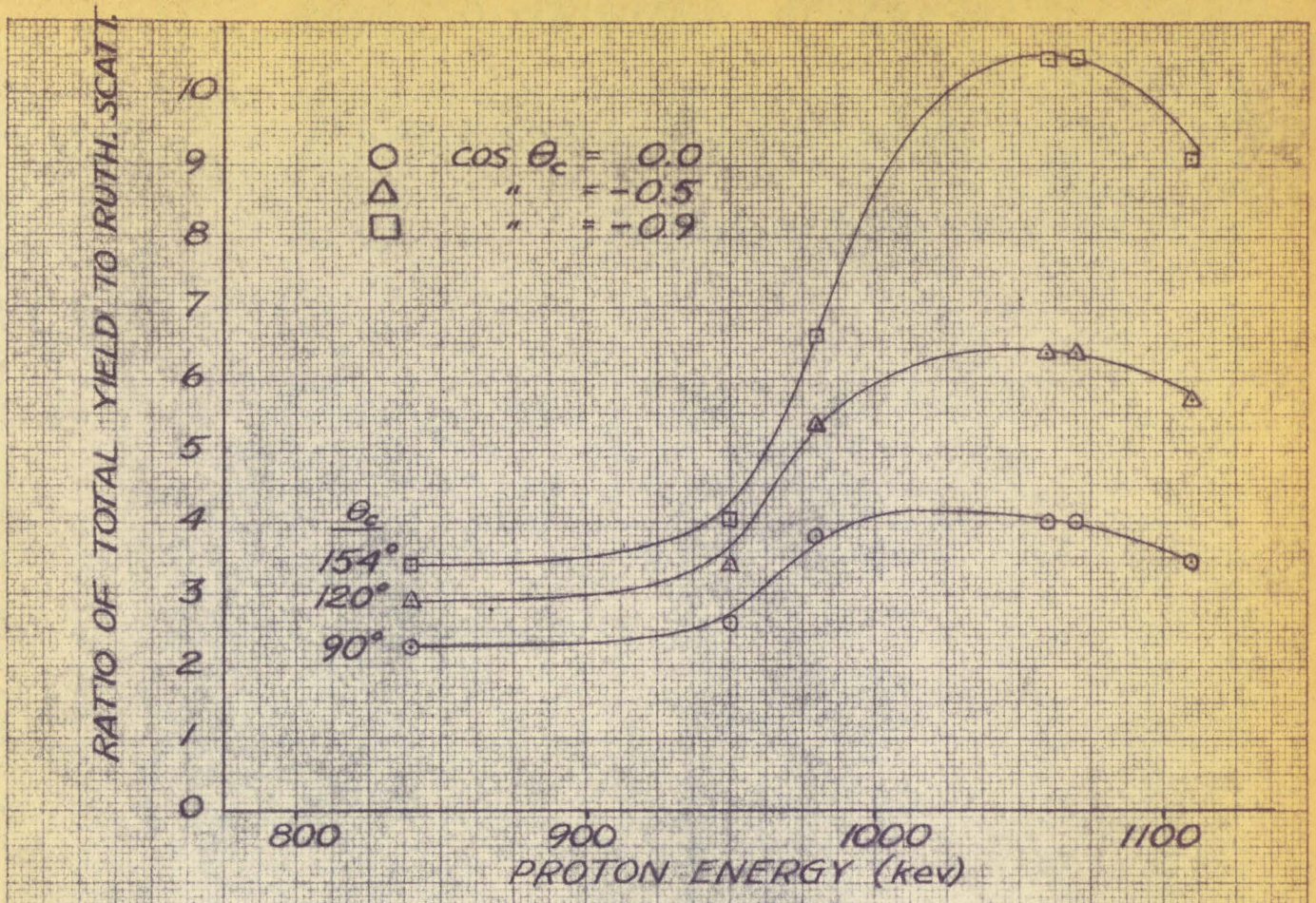
RATIO OF TOTAL YIELD TO RUTH. SCATT.
10
9
8
7
6
5
4
3
2
1
0
○ cos θc = 0.0
△ " = -0.5
□ " = -0.9
θc
154°
120°
90°
800
900
1000
1100
PROTON ENERGY (kev)

FIG. 11

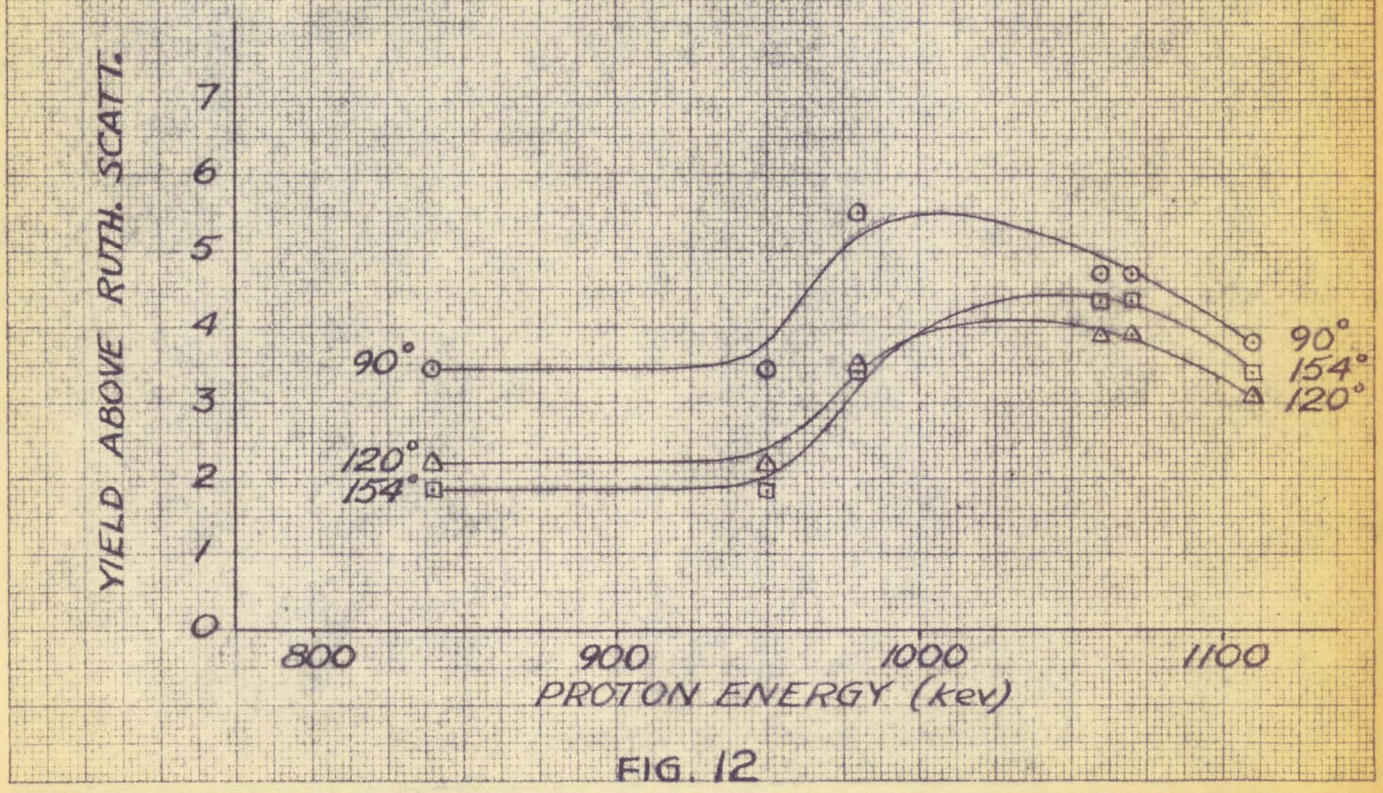
YIELD ABOVE RUTH. SCATT.
7
6
5
4
3
2
1
0
90°
120°
154°
90°
154°
120°
800
900
1000
1100
PROTON ENERGY (kev)

FIG. 12

$Be^9(p,\gamma)B^{10}$

RANGE DISTRIBUTION AT $\theta_c = 90°$

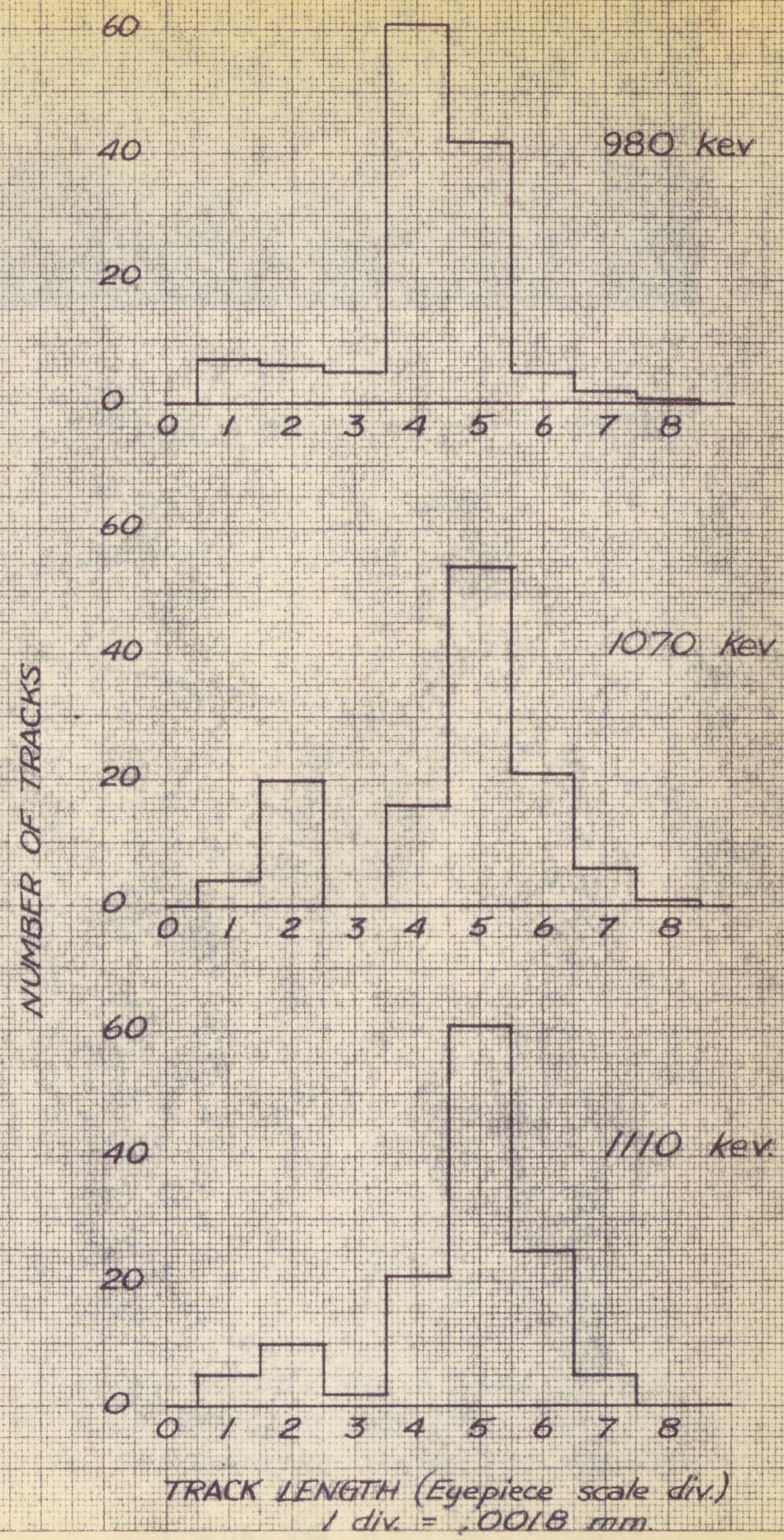

FIG. 13

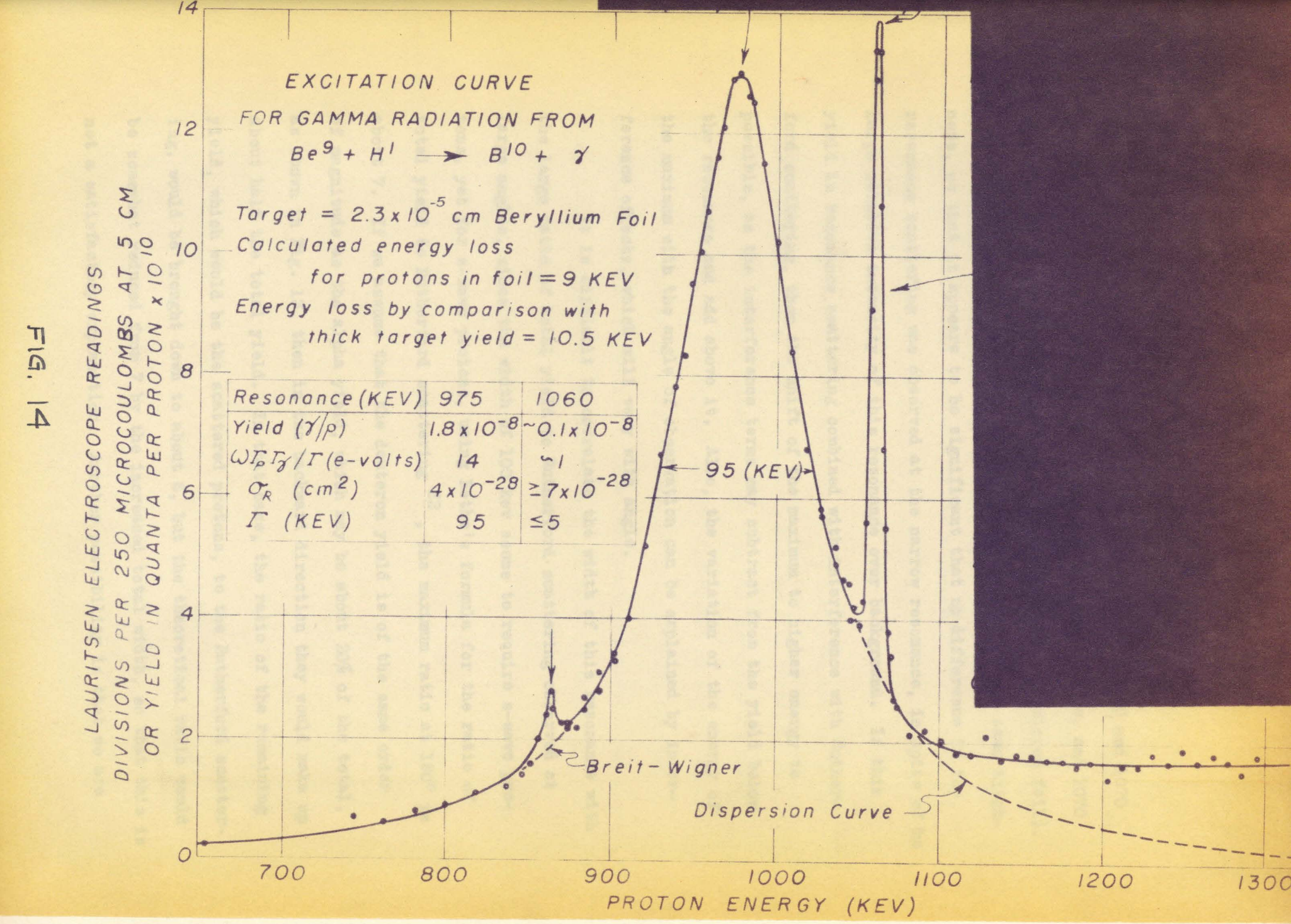

Resonance (KEV)	975	1060
Yield (γ/p)	1.8×10^{-8}	$\sim 0.1 \times 10^{-8}$
$\omega\Gamma_p\Gamma_\gamma/\Gamma$ (e-volts)	14	~ 1
σ_R (cm^2)	4×10^{-28}	$\geq 7 \times 10^{-28}$
Γ (KEV)	95	≤ 5

FIG. 14

the narrow resonance is observed, as the two curves for 1060 and 1070 kev are indistinguishable, although 1060 is definitely below, and 1070 kev is at the maximum of the narrow resonance (for the .23 micron foil). Fig. 14 shows the γ-ray yield from a beryllium foil of the same thickness, so that it appears to be significant that no difference in the resonance scattering was observed at the narrow resonance, in spite of the large relative intensity of this resonance over background. If this yield is resonance scattering combined with interference with Rutherford scattering, then the shift of the maximum to higher energy is possible, as the interference terms may subtract from the yield below the resonance and add above it. Also, the variation of the energy of the maximum with the angle of observation can be explained by interference effects, which will vary with angle.

It is difficult to correlate the width of this resonance with the large ratio of total yield to Rutherford scattering observed at large angles, since the width of 100 kev seems to require s-wave protons, yet for s-wave protons, using Bethe's formula for the ratio of total yield to Rutherford scattering [32], the maximum ratio at 180° is about 7. If we assume that the deuteron yield is of the same order of magnitude as the alpha yield, which may be about 20% of the total, as shown in Fig. 13, then in the backward direction they would make up about half the total yield. In that case, the ratio of the remaining yield, which would be the scattered protons, to the Rutherford scattering, would be brought down to about 6, but the theoretical ratio would be somewhat reduced from 7 by the increased total width, so that this is not a satisfactory explanation. Another possibility is that we are

dealing with more than one resonance in the emission of heavy particles, or that there is a strong background in addition to the resonance, which would change the critical quantities sufficiently to account for this effect with resonance scattering of s-wave protons. It may also be that the broad γ-ray resonance is due to p-wave protons, and that it is the large width which needs to be explained.

The author is indebted to Dr. C. C. Lauritsen and Dr. W. A. Fowler for much helpful advice and assistance in this research, to Dr. T. Lauritsen for assistance in operating the electrostatic generator, and to Dr. R. F. Christy for helpful discussion on the theoretical aspects of the problems. This work was carried out under contract of the laboratory with the Office of Naval Research; and under a pre-doctoral fellowship grant to the author from the National Research Council.

References

1. F. Kirchner: Phys. Zeits. 34, 777 (1933)

2. J. Giarratana, C. G. Brennecke: Phys. Rev. 49, 35 (1936)

3. A. E. Kempton, B. C. Browne, R. Maasdorp: Proc. Roy. Soc. 157, 386 (1936)

4. H. Neuert: Phys. Zeits. 38, 122 (1937)

5. H. Neuert: Phys. Zeits. 38, 618 (1937)

6. H. Neuert: Zeit. f. Tech. Physik 19, 576 (1938)

7. R. O. Haxby, J. S. Allen, J. H. Williams: Phys. Rev. 53, A921 (1938)

8. A. Ellett, R. D. Huntoon: Phys. Rev. 59, A87 (1938)

9. R. O. Haxby, J. S. Allen, J. H. Williams: Phys. Rev. 55, 140 (1939)

10. H. Neuert: Ann. d. Physik 36, 437 (1939)

11. E. Gerjuoy: Phys. Rev. 58, 503 (1940)

12. C. L. Critchfield, E. Teller: Phys. Rev. 60, 10 (1941)

13. E. Eisner: Phys. Rev. 65, 85 (1944)

14. G. Breit, B. T. Darling: Phys. Rev. 71, 402 (1947)

15. R. D. Huntoon, A. Ellett, D. S. Bayley, J. A. Van Allen: Phys. Rev. 58, 97 (1940)

16. H. P. Manning, R. D. Huntoon, F. E. Myers, V. J. Young: Phys. Rev. 61, 371 (1942)

17. W. E. Bennett, C. E. Mandeville, H. T. Richards: Phys. Rev. 69, 418 (1946)

18. V. J. Young, A. Ellett, G. J. Plain: Phys. Rev. 58, 498 (1940)

19. C. D. Swartz, H. H. Rossi, B. Jennings, D. R. Inglis: Phys. Rev. 65, 80 (1944)

20. W. B. McLean, A. Ellett, J. A. Jacobs: Phys. Rev. 58, 500 (1940)

21. H. H. Rossi, C. D. Swartz: Phys. Rev. 65, 83 (1944)

22. J. Chadwick, A. N. May, T. G. Pickavance, C. F. Powell: Proc. Roy. Soc. 183, 1 (1944)

23. M. S. Livingston, F. Genevese, E. J. Konopinski: Phys. Rev. 51, 835 (1937)

24. M. Ostrofsky, G. Breit, D. P. Johnson: Phys. Rev. 49, 22 (1935)

25. L. H. Rumbaugh, R. B. Roberts, L. R. Hafstad: Phys Rev. 54, 657 (1938)

26. R. F. Christy, S. Rubin: Phys. Rev. 71, A275 (1947)

27. L. J. Haworth, L. D. P. King: Phys. Rev. 54, 38 (1938)

28. J. F. Streib, W. A. Fowler, C. C. Lauritsen: Phys. Rev. 59, 253 (1941)

29. The thin beryllium foils were made by Dr. H. Bradner, of the Radiation Laboratory, Berkeley.

30. L. I. Schiff: Phys. Rev. 70, 891 (1946)

31. C. C. Lauritsen, T. Lauritsen, W. A. Fowler: Phys. Rev. 71, A279 (1947)

32. H. A. Bethe: Rev. Mod. Phys. 9, 176 (1937) - Formula 625